Reduction of ionosphere divergence error in GPS code measurement smoothing by use of a non-linear process

Shiladitya Sen & Jason H. Rife
Tufts University

>> Accepted Article <<

CITATION:
S. Sen and J. Rife (2012). Reduction of ionosphere divergence error in GPS code measurement smoothing by use of a non-linear process. *IEEE Transactions on Aerospace and Electronic Systems*, 48(2), pp. 981-990. First published under the same title in *Proc. ION/IEEE Position, Location, and Navigation Symposium (PLANS)*, 2008, Monterey, CA. DOI: 10.1109/PLANS.2008.4570020.

CORRESPONDING AUTHOR:
Jason Rife
jason.rife@tufts.edu

Reduction of Ionosphere Divergence Error in GPS Code Measurement Smoothing by Use of a Non-Linear Process

Shiladitya Sen, Tufts University
Jason Rife, Tufts University

Abstract – This paper develops a single-frequency filter for smoothing GPS code measurements using a nonlinear method. The method zeroes steady-state divergence errors caused by ionospheric storms. The filter has significant potential to improve the availability of safety-critical differential GPS systems such as Ground-Based Augmentation Systems (GBAS). These systems, of which the Local Area Augmented System (LAAS) is one example, typically rely on a Hatch Filter for code smoothing. Although the Hatch filter offers excellent noise reduction and ease of implement under nominal conditions, the filter amplifies ionosphere errors under rare, anomalous storm conditions. Our method generalizes the Hatch Filter by adding a correction term which is computed through a nonlinear process. The nonlinear process detects high ionosphere-delay gradients and estimates the appropriate correction term for the Hatch Filter. Experimental trials indicate that the nonlinear filter not only zeroes steady-state divergence but also reduces maximum transient errors by 0-25% relative to the Hatch Filter without impacting filter noise under nominal conditions.

I. INTRODUCTION

The ionosphere is a dispersive medium that forms a part of earth's atmosphere extending approximately from 50 Km to 1000 Km above earth's surface. It is characterized by the presence of free electrons caused by the ionization of gas molecules by solar radiation [1]. The speed of a radio signal through the ionosphere is dependent on the total number of free electrons along its path, a quantity known as total electron content (TEC). Due to the free electrons there is an error in GPS range estimation, known as ionospheric delay. High solar activity may cause the TEC to change rapidly in space and time giving rise to high gradients of ionospheric delay. This event is generally referred to as an ionospheric storm. Several such storms have been reported in recent years [2]. During an ionospheric storm a LAAS user may suffer divergence bias errors that differential corrections cannot remove. These bias errors result from the integration of ionospheric code-carrier divergence by the Hatch Filter, commonly used for code smoothing. In its steady state, these biases can be above 10m for the worst ionospheric storms on record. Moreover, because the Hatch Filter has "memory," the divergence error remains in the system even after the LAAS receiver is no longer exposed to the ionospheric storm. In this sense, bias errors due to anomalous code-carrier divergence severely threaten LAAS integrity.

In principle, ionospheric divergence errors could be eliminated entirely using two GPS frequencies [3, 4]. These approaches are not yet viable for civil aviation applications, as the second GPS frequency (L2) does not fall in a protected Aeronautical Radio Navigation Service (ARNS) band and as the proposed third GPS frequency (L5) will not be widely available until well into the next decade.

To enable a more rapid deployment of LAAS, single-frequency monitoring and filtering algorithms have been proposed. For instance, single-frequency monitors have been designed to detect both code-carrier divergence [5] and differences in accumulated divergence for filters with different time constants [6, 7]. The risk posed by code-carrier divergence can be further mitigated by redesigning the code-smoothing Hatch Filter to reduce the error induced by an anomalous ionospheric storm [8].

The duration that steady-state errors persist has not generally been considered in the analysis of these proposed ionosphere mitigation strategies for LAAS. Yet the duration that large errors persist is directly related to the risk that these errors result in an integrity fault. To optimize LAAS availability, it may be desirable to modify standard availability modeling tools [9, 10] to account for the increased risks associated with large persistent errors.

To minimize the risks associated with persistent ionosphere divergence errors, we propose a single-frequency filter for which the steady-state divergence error decays to zero. This filter consists of a standard Hatch Filter and a nonlinear divergence estimation algorithm which provides a Hatch Filter correction term. The next section details the advantages of using a nonlinear algorithm for divergence estimation. Next, the proposed nonlinear algorithm is validated using a combination of simulated ionosphere anomalies and archived GPS data available through the website for the Continuously Operating Reference Stations (CORS) network. Finally, the paper concludes with a discussion of the possible implications of this filter for LAAS.

II. APPROACH

A. Ionosphere Storm Model

Ionosphere storm models have been developed by several researchers [2, 9, 10] to support safety analyses of precision landing using LAAS. These models are based on observations of large ionosphere walls detected with arrays of GPS receivers positioned across North America. The standard ionosphere storm model consists of a steep traveling wavefront between regions of low and high ionosphere delay. The wavefront is modeled as a piecewise linear curve described by three parameters: a specified ionosphere delay gradient, a wavefront speed and a wavefront width. This standard model is illustrated for representative parameters in Fig. 1. This figure shows a potential threat scenario when the ionosphere storm only affects the airborne LAAS receiver and not the stationary receiver at the LAAS reference station.

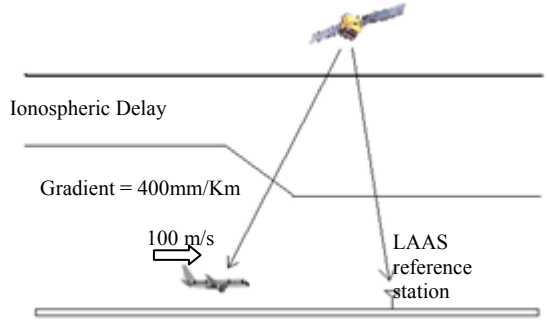

Figure 1: Model of an Ionospheric storm

For the purposes of safety analysis, storm parameters (delay gradient, wavefront speed and width) are bounded by a threat space derived from GPS data. On a nominal day the ionospheric delay varies little over large regions, changing gradually at about 1-2 mm/km. These gradients are not a threat to LAAS as they are also seen by the LAAS reference station which suitably mitigates the errors by differential corrections. Due to an ionospheric storm the ionospheric delay can have a high gradient of 300 - 400 mm/km as seen in fig. 2. This ionospheric wavefront can have a speed of 0 – 1000 m/s.

Slower moving ionospheric wavefronts are particularly dangerous because they result in an increased risk that the LAAS reference station will never see the storm and hence will never detect it [9]. In one of the worst cases a slow storm is only seen by the aircraft and not the ground station, as shown in fig. 1. In this scenario the airborne LAAS receiver experiences two errors, the ionospheric delay and the divergence error. The ionospheric delay error is the difference between the delay observed at the aircraft and that observed by the reference station, as illustrated in the figure. This error always grows smaller as the aircraft approaches the ground station. Additional error is introduced when the Hatch Filter processes the opposing ionosphere delays on the code and carrier signals. Filtering causes the receiver (in this example the aircraft receiver) to track the rapidly changing storm-front delay with a bias. The divergence bias error B is illustrated in fig. 2 as the difference between a raw code signal (featuring a steep ionosphere gradient) and the output of a Hatch Filter applied to that code. The steady-state divergence error remains in the system even after the airborne receiver is no longer exposed to the ionospheric delay gradient. Because large divergence bias errors do not disappear when the aircraft approaches the ground reference station, they represent a significant integrity threat for precision landing applications.

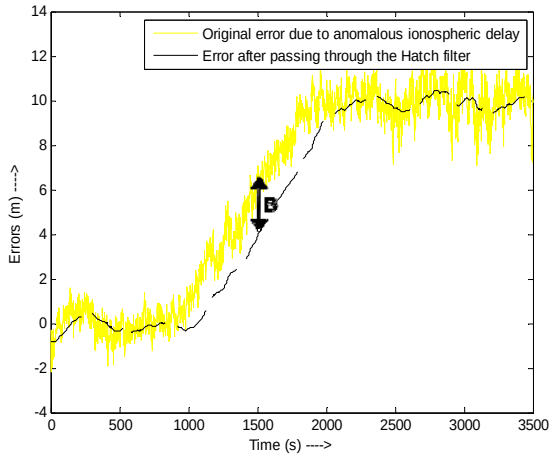

Figure 2: Ionospheric delay and divergence error

B. Zeroing the Steady-State Error

To enhance safety for safe aircraft landing applications, the challenge is to identify a class of filters that can eliminate steady-state error without degrading nominal noise and without increasing the maximum transient divergence error. It is not difficult to design a low-pass filter for the code that will have a zero steady-state divergence error. In concept the algorithm simply needs to estimate the ionosphere gradient and subtract off the resulting divergence error. However subtracting the steady-state error reduces attenuation of high frequency noise. If the filter time constant is adjusted to maintain a desired level of noise attenuation, then the maximum transient error increases for any linear filter implementation [8]. Thus the steady-state error cannot be removed from a linear filter without sacrificing either nominal noise performance or transient bias performance during an ionosphere storm. The goal of this filter is to introduce a nonlinear divergence-eliminating filter that overcomes these limitations of linear filters.

One of the reasons for the poor performance of linear filters is that that they inherently treat the ionospheric delay ramp as a straight line and ignore the starting time of the ionospheric ramp, as shown in fig. 3. This procedure of ionospheric gradient estimation is accurate over long times but is inaccurate shortly after the starting time of the event. In fact, the ionosphere event is better modeled as a piecewise linear phenomenon than a purely linear one. Linear filters, which assume purely linear rather than piecewise linear divergence, have large transient errors as a result.

We propose a nonlinear estimation approach that treats the ionosphere event as a piecewise linear ramp rather than a purely linear ramp of infinite extent. A two slope piecewise linear model enables the identification of the starting time (or transition time) for the ionospheric anomaly and the estimation of distinct ionospheric gradient on either side of this transition. The piecewise linear model overcomes the limitation of the purely linear model in that it provides a much more accurate representation of the ionosphere delay changes near the transition.

Although real ionospheric events may not necessarily have a sharply defined start time, the two-slope approach still provides a relatively accurate model of the ionosphere, as can be observed in fig. 3. It should also be noted that under nominal conditions (when there is no event), the slopes of both the lines tend to be the same and the nonlinear filter acts as a linear filter.

Implementing ionospheric divergence estimation using a piecewise linear curve, our algorithm can determine a correction term that eliminates the steady-state divergence bias from the output of a standard Hatch Filter. This is inherently a non-linear process because the filter adapts to the starting time of the ionospheric anomaly which is a variable and is computed at each instant. We call this alternative to the baseline Hatch Filter the Non-Linear Divergence Elimination (NLDE) filter algorithm.

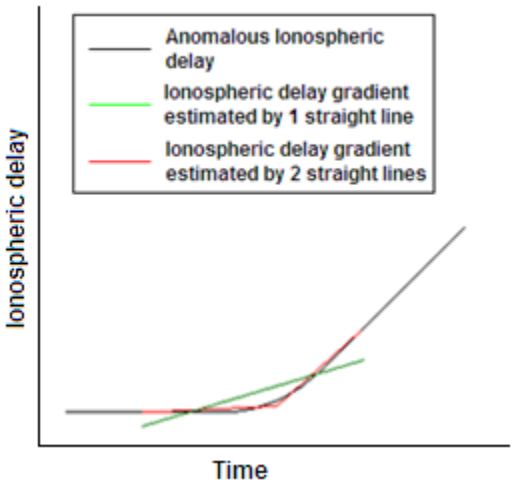

Figure 3: Estimation of anomalous Ionospheric gradient using 1 line method and 2 line method

III. NLDE Filter Algorithm

This section provides a mathematical development for the proposed nonlinear filtering strategy. Essentially, the NLDE filter generalizes a Hatch Filter by introducing a correction term to compensate for the lag that Hatch Filters experience due to ionospheric storms. The NLDE block diagram is given in fig. 4. Essentially the Hatch Filter is computed normally while the ionospheric delay is calculated in parallel. As shown in the figure, the nonlinear divergence estimator block takes as an input a noisy estimate of the ionosphere delay for a particular satellite (subject to an integer bias associated with the carrier phase). This block fits a piecewise linear ionosphere gradient model to recent data. The gradient is subsequently used to determine the steady-state divergence bias, illustrated earlier in fig. 1. The steady-state divergence bias extrapolated from the current ionosphere time derivative is labeled

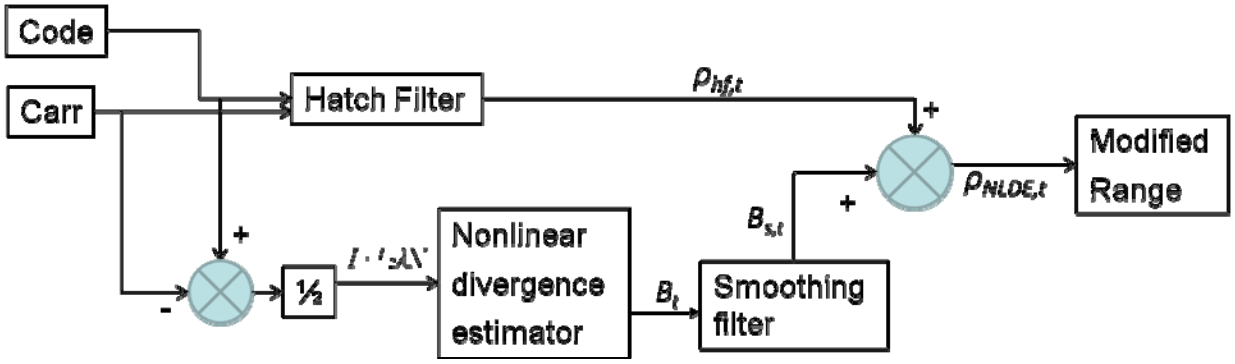

Figure 4: Block diagram of the NLDE filter

B_t. This steady-state bias estimate is passed through a smoothing filter and subsequently added as a correction to the Hatch Filter output. The remainder of this section details each element of the block diagram shown in fig. 4.

The baseline Hatch Filter illustrated in fig. 4 is implemented with the following equation designed to smooth the code measurement using the carrier measurements.

$$\rho_{hf,t} = \frac{1}{M}\rho_t + \left(1 - \frac{1}{M}\right)\left(\rho_{hf,t-1} + \phi_t - \phi_{t-1}\right) \quad (1)$$

ρ_t = code measurement at epoch t
ϕ_t = carrier measurement at epoch t
$\rho_{hf,t}$ = carrier smoothed code at epoch t
M = length of the Hatch Filter

The ionospheric delay in code measurements is exactly opposite of that in carrier measurements. Keeping the key components and neglecting errors from multipath, the code and carrier signal can be written as below.

$$\rho_t = r_t + c_t + I_t + T_t + \epsilon \quad (2)$$
$$\phi_t = r_t + c_t - I_t + T_t + \lambda N \quad (3)$$

r_t = true range at epoch t
c_t = clock biases at epoch t
I_t = ionospheric delay at epoch t
T_t = tropospheric delay at epoch t

The true range is represented by r_t at epoch t. The product of the wavelength of GPS radiowaves λ and the integer ambiguity N introduces a bias in the carrier phase pseudorange measurement. The diffuse multipath and thermal noise is denoted by ε.

A model of the Hatch Filter divergence bias can be defined using the above equations. Essentially the divergence bias b_t is the additional error in the smoothed estimate of true range other than the ionospheric delay and clock biases. Lower case notation (b_t) is used for the transient bias to distinguish it from the steady-state error (B_t), for which upper case notation is used.

$$b_t = \rho_{hf,t} - r_t - I_t - c_t - T_t \quad (4)$$

Substituting equation (2) and (3) in (1) and subtracting r_t+I_t+c_t+T_t, from both sides we get the following relation.

$$b_t = \left[\frac{(M-1)b_{t-1} - 2(M-1)(I_t - I_{t-1})}{M}\right] + \frac{\varepsilon}{M} \quad (5)$$

To obtain the steady-state divergence bias B_t we observe that b_t should be same as b_{t-1} when steady state is reached. On rearranging we obtain the following equation, in which the negative sign signifies that B_t is a delay. Note that the steady-state bias is considered to be a function of time, rather than a constant value, because the steady-state calculation extrapolates the ionosphere change rate assessed at the current epoch t.

$$B_t = -2(M-1)(I_t - I_{t-1}) + \varepsilon \quad (6)$$

The primary function of the nonlinear divergence estimator block in fig. 4 is to estimate the steady-state delay B_t given by the above equation.

In our present implementation, the nonlinear divergence estimation block is implemented as an exhaustive search over all possible starting times for the anomalous ionosphere event (within a window of

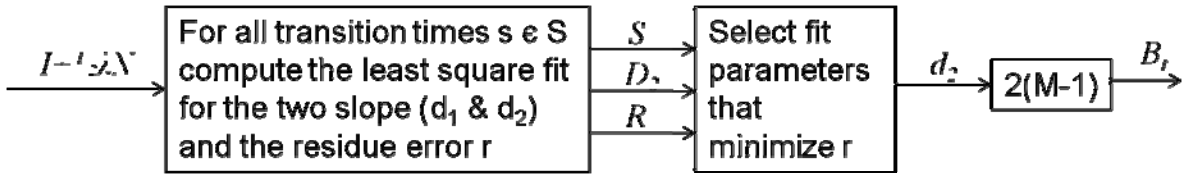

Figure 5: Block diagram of the nonlinear divergence estimator in the NLDE filter

buffered data). This exhaustive search strategy is summarized in fig. 5. The search process considers all possible piecewise linear anomaly models which fit within a data buffer which holds in memory the last P measurements. In concept, the anomaly transition could occur at any epoch within the buffer, noting that a transition occurring at either the edge of the buffer provides an equivalent model to a transition occurring outside the buffer. In practice, the estimation of the steady-state bias is highly sensitive to noise in estimation of the slope of the second segment of the piecewise model. To ensure enough measurements to mitigate noise in this estimate, the transition time is restricted to ensure that at least a minimum of L measurements remain after the transition. Thus the exhaustive search considers all start times s in the set $S \in \{1 \le s \le P\text{-}L\}$.

For each possible transition time, s, the nonlinear divergence estimator computes a least squares fit for each of the two segments of the piecewise linear ionosphere delay model. The two straight lines are fit independently. The process begins by identifying a slope and an offset for the first segment of the model (d_1 and e, respectively). These parameters are determined to provide a best fit to the NLDE input data, $y = ½(\rho - \phi) = I + ½\lambda N$. The offset parameter e compensates for both the raw ionosphere delay and the unknown integer ambiguity in the carrier phase.

$$\begin{bmatrix} d_1 \\ e \end{bmatrix} = \begin{bmatrix} 1 & \sum_1^s t_i \\ \sum_1^s t_i & \sum_1^s t^2 \end{bmatrix}^{-1} \begin{bmatrix} \sum_1^s y_i \\ \sum_1^s t_i y_i \end{bmatrix} \qquad (7)$$

Next, the slope d_2 of the second segment can be found in a similar way. The second straight segment of the piecewise model is constrained, however, to start from the last point of the first segment. The second segment slope values d_2 for each transition time s are compiled into a vector called D_2. For each start time the corresponding residual errors r are compiled into a companion vector R. The best fit is determined as the model with the lowest residual (i.e. the model corresponding to the minimum element of R). In our implementation, the residual r was computed using a one-norm of the curve-fit error, rather than the two-norm conventionally associated with a least squares fit. The use of the one-norm for comparison was intended to provide an additional measure of robustness for the curve fit, since the least squares and residual minimization processes essentially force both the one and two-norms of the residual to be small.

The NLDE block, shown in fig. 4, outputs an estimate of the steady-state divergence bias B_t. This output value is determined from (6) using the second-segment slope d_2 for the best-fit piecewise model. The change in ionosphere delay between successive epochs is approximately equal to the product of the ionosphere derivative d_2 and the sample rate Δt. Hence the steady-state divergence bias of (6) may be rewritten as follows.

$$B_t = 2(M-1)d_2\Delta t \qquad (8)$$

To minimize the noise added to the system, B_t is smoothed by a first order IIR smoothing filter of length F.

$$B_{s,t} = \frac{1}{F}B_t + \left(1 - \frac{1}{F}\right)B_{s,t-1} \qquad (9)$$

The smoothed delay $B_{s,t}$ is added to the Hatch Filter output $\rho_{hf,t}$ as shown in the equation below. In the absence of ionospheric delay gradients the correction term $B_{s,t}$ tends to zero and the NLDE filter reduces to a Hatch Filter.

$$\rho_{NLDE,t} = \rho_{hf,t} + B_{s,t} \qquad (10)$$

IV. NLDE PERFORMANCE

This section describes the performance of the NLDE algorithm based on a combination of theory

and application of the filter to representative GPS data. Performance is considered for two case studies, a first which compares the Hatch and NLDE filters for a matched Hatch Filter length *M* and a second which compares the two filters for a matched output noise variance.

The first study compares a particular implementation of the NLDE filter (with parameters P = 300, L = 60, M = 70, F = 200) to a baseline Hatch Filter with the same time constant (M = 70). As compared with the baseline Hatch Filter, the nonlinear correction term helps the NLDE filter to achieve zero steady-state bias error and more than a 50% reduction of the maximum transient error. However, the addition of the bias compensation term worsens the noise characteristics of the NLDE output.

To demonstrate these results, a simulation can be performed that isolates the divergence effects from the nominal noise. The results of the noise-free simulation are illustrated in fig. 6. The modeled ionospheric delay input is shown in the inset of fig. 6 with a gradient of 0.04m/s. This ionosphere time-derivateive was chosen to correspond to a severe threat with a storm spatial gradient of 400 mm/km and an aircraft velocity of 100 m/s. The maximum transient error due to divergence for the NLDE filter was only 2.55m compared to that of 5.56m of Hatch Filter. Also the exposure to the bias was cut down to only about 400 epochs after which the divergence error approached a steady state of zero.

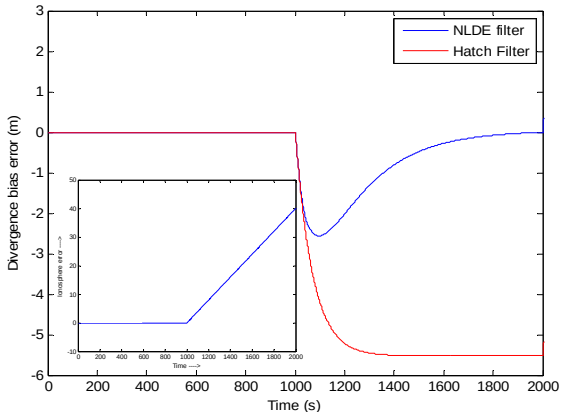

Figure 6: Comparison of NLDE and Hatch Filter on ionospheric delay model

The ability of the NLDE filter to attenuate nominal noise can be assessed by applying the filter to a representative GPS data set. Since the NLDE filter adds a noisy correction term to a Hatch Filter, its output noise variance is expected to increase. The increase is only a moderate change, as illustrated in fig. 7 where the NLDE filter output on a nominal day is comparable to that of the Hatch Filter. Specifically, the 1σ noise level increased to 0.34m (for the NLDE) from 0.24m (for the Hatch Filter alone). In both cases, the input signal had a 1σ noise level of 0.66m. Noise levels were estimated using a Code-Minus-Carrier approach (with a fifth-order curve fit introduced to remove the nuisance parameter associated with the ionosphere and the integer ambiguity: $2I - \lambda N$).

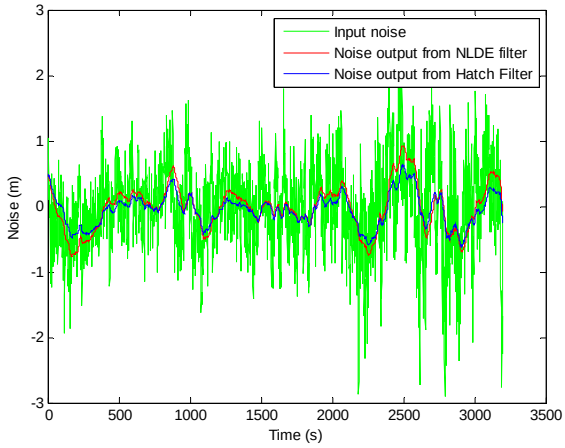

Figure 7: Noise characteristic comparison of NLDE filter and Hatch Filter

The decomposition of NLDE performance into a distinct ionosphere anomaly response (fig. 6) and a nominal noise response (fig. 7) is not a complete description, since the superposition principle does not necessarily hold for nonlinear systems. Accordingly, the performance of the NLDE filter can be verified by analyzing its response to a combined input signal consisting of nominal noise plus the modeled ionospheric storm. Fig. 8 shows the response for this case. The illustrated results are representative and suggest that, in fact, superposition is a reasonable approximation for analysis of the NLDE.

A second case compares an NLDE filter (with parameters P = 300, L = 60, M = 70, F = 200) to a Hatch Filter with a matched level of output noise (M = 36). It is observed in this case that the NLDE filter is able to achieve both a smaller maximum transient error than the Hatch Filter and a zero steady-state error. A comparison of the two filters with matched output noise is also illustrated in Fig. 8. The next section considers uses many data sets to validate this performance comparison of the NLDE and Hatch Filters.

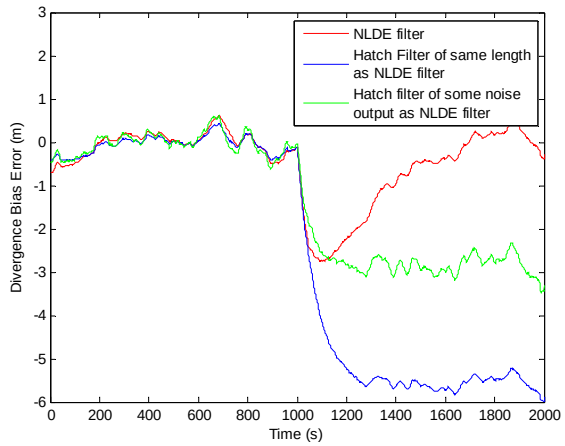

Figure 8: Comparison of NLDE and Hatch Filter to combined nominal noise and ionospheric storm model

V. Data Validation

Analysis of GPS data confirms that the NLDE filter outperforms the Hatch Filter when the Hatch Filter time constant ($M \cdot \Delta t$) exceeds 50s. To demonstrate this result, divergence errors were compared for NLDE filters and Hatch Filters of the same noise characteristic Γ (defined as the ratio of output noise variance to input noise variance). The filters were tested on data archived at a frequency of 1 Hz for all satellites visible during the first hour of August 28, 2006 as observed at the Oakland, CA reference station designated ZOA1. This station belongs to the Wide Area Augmentation System (WAAS) network. The ZOA1 data are also logged in the Continuously Operational Reference Station (CORS) database.

The performance of the NLDE filter was found to dependent on its four parameters. The four parameters are the buffering time P, the minimum permissible length of the second piecewise segment L, the Hatch Filter length M and the smoothing filter length F. The parameters chosen for analysis in this paper are given in table 1. Values were selected empirically to provide reasonable performance. Further performance enhancement may be possible through a formal parameter optimization.

No. of buffered points (P epochs)	Minimum length (L epochs)	Hatch Filter length (M epochs)	Smoothing filter length (F epochs)
300	60-90	70-120	200-800

Table 1: Analyzed parameter space

Because superposition is not guaranteed for nonlinear filters, the maximum transient error of the NLDE filter was calculated in a statistical sense. To calculate the maximum transient error, the ionospheric storm was placed at randomized starting points in the GPS data sets. The maximum transient error was recorded as the maximum divergence error in a window of ten epochs centered about the point of the theoretical maximum transient for the zero noise case. This window accommodated for small shifts, if any, in the occurrence of maximum transient divergence error due to the nonlinearity of the filter. The average of all the divergence errors, each corresponding to a different random starting point, is reported as a statistical estimate of the NLDE maximum transient error.

For a fixed level of output noise, the maximum divergence bias of the NLDE filter was found to be lower than that of the Hatch Filter for the ranges of NLDE parameters considered. Fig 9 shows results for PRN 27, including one-sigma error bars for the NLDE filter results. The plot is representative of most of the other satellites analyzed. The plot shows that the maximum transient error (vertical axis) is lower for the NLDE (dotted line) than for the Hatch Filter (solid line) across a wide range of output variance levels (horizontal axis). Although not shown in the illustration, the NLDE also offers the additional advantage of zero steady-state divergence error. It should be noted here that more than one set of parameters (P, L, M, F) can be employed to achieve a particular level of output noise The dotted red curve in fig. 9 represents the best parameter set studied for each output-to-input noise ratio Γ.

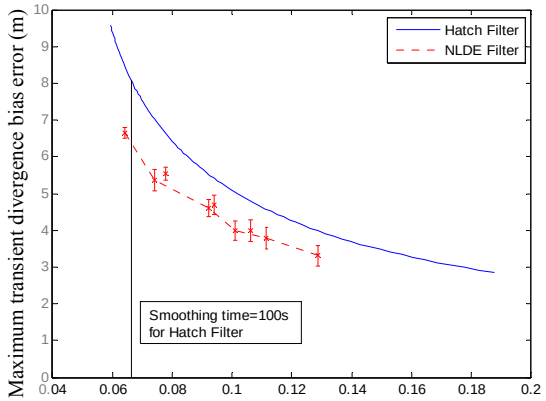

Figure 9: Maximum divergence bias error as a function of noise characteristic Γ for NLDE and Hatch Filter

The weakest NLDE performance was observed for a high elevation satellite, PRN 11. For this satellite, the NLDE filter was only marginally better than the Hatch Filter. In fact, as illustrated in fig. 10 the NLDE filter performs worse than the Hatch Filter for values of Γ more than 0.22. These values translate to Hatch Filter time constants of 50 s or below. These results imply that the NLDE does not perform unambiguously better than the Hatch Filter when the required level of noise attenuation is small. Given that LAAS generally operates with Hatch Filter time constants of more than 60s, the NLDE filter appears to outperform the Hatch Filter in the range relevant for the LAAS application..

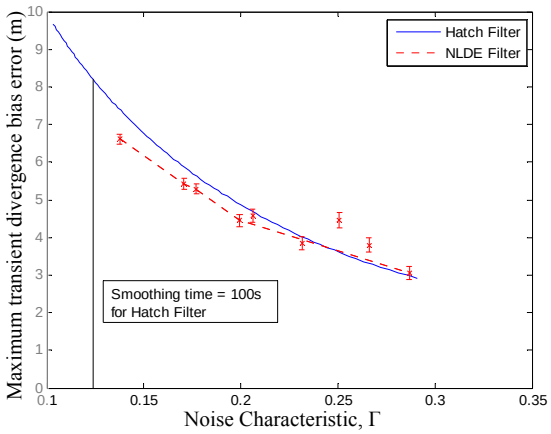

Figure 10: Maximum divergence bias error as a function of output-to-input noise variance ratio Γ for the NLDE and Hatch Filters - Worst case

VI. Discusion

For a practical implementation of the NLDE filter, several further issues should be considered. These issues include the computational processing requirements of the method, its dynamic response and settling time, and the generalization of the validation process.

The computational time requirement for the NLDE algorithm is much higher than that for the Hatch Filter on account of the exhaustive search for the transition time between the two segments of the piecewise linear model. The NLDE algorithm computation cost is order O(P), i.e. the cost is proportional to the buffer length. For offline tests, the time taken to analyze each epoch was approximately 0.1 seconds per satellite using a 1.6GHz laptop. Several numerical strategies might be examined in the future to ensure faster convergence in the NLDE block while finding the best curve fit.

The settling time to attain zero steady-state divergence bias varied from 300 epochs to 900 epochs. The settling time was found to be dependent on the choice of parameters, especially on F. Future work will consider alternative smoothing filters with faster transient responses in place of the current IIR filter.

Additional validation tests for the NLDE method should also be considered in the future. Because of the nonlinear nature of the NLDE filter design and the corresponding fact that superposition does not hold, additional ionosphere storm scenarios should be evaluated. The previous section focused on analysis of a 0.04 m/s ionosphere gradient injected into GPS data taken under nominal conditions. The NLDE filter gives similar reduction of divergence bias for an 0.002 m/s modeled ionosphere gradient. Other modeled gradient levels should also be analyzed, as well as data acquired during actual ionosphere storm events.

VII. Summary and Conclusions

The Hatch Filter, which leverages carrier phase data to smooth GPS code pseudoranges, introduces significant divergence biases during anomalous ionosphere storms. These biases are not necessarily canceled by differential corrections broadcast from a local-area reference station. If unchecked, these biases attain high values in steady state and threaten the integrity of GPS landing systems like LAAS. This paper provides an alternative filter to reduce the time of exposure of aircraft to hazardous ionosphere storms. A nonlinear filter named the NLDE filter was designed based on the popularly accepted piecewise-linear ionospheric storm model. The NLDE estimates the start time of an ionospheric anomaly and smoothes code measurements independently on either side of the start time. The filter accordingly attains zero divergence error in steady state without increasing the transient divergence error.

For the range of parameters considered the NLDE filter not only successfully reduced the time of exposure to ionospheric storm biases, it also reduced the maximum transient divergence error by 0 to 25% as compared to a Hatch Filter with the same level of output noise. The excellent performance of the NLDE filter comes at a mild computational cost. Refined numerical methods have great potentially to make the algorithm faster for real-time applications.

REFERENCES

[1] P. Misra and P. Enge, *Global Position System: Signals, Measurements, and Performance*. Ganga-Jamuna Press, 2006.

[2] M. Luo, S. Pullen, A. Ene, D. Qiu, T. Walter, and P. Enge, "Ionosphere threat to LAAS: updated model, user impact, and mitigations", *Proceedings of the Institute of Navigation's ION-GNSS 2004*, pp. 2771-2785.

[3] H. Konno, S. Pullen, J. Rife, and P. Enge, "Evaluation of Two Types of Dual-Frequency Differential GPS Techniques under Anomalous Ionosphere Conditions", *Institute of Navigation's National Technical Meeting*, January 2006.

[4] P. Hwang, G. McGraw, J. Bader, "Enhanced Differential GPS Carrier-Smoothed Code Processing Using Dual-Frequency Measurements," *Navigation*. Vol. 46, No. 2, summer 1999, pp. 127-137.

[5] D. V. Simili, B. Pervan, "Code-Carrier Divergence Monitoring for the GPS Local Area Augmentation System", *Position, Location, And Navigation Symposium, 2006 IEEE/ION,* 25-27 April 2006, pg 483-493.

[6] T. Walter, "The Effects of Large Ionospheric Gradients on Single Frequency Airborne Smoothing Filters for WAAS and LAAS", *Institute of Navigation's National Technical Meeting*, January 2004.

[7] T. Murphy, M. Harris, Boeing Commercial Airplanes, "More Ionosphere Anomaly Mitigation Considerations for Category II/III GBAS", *ION GNSS 2007.*

[8] J. Rife, S. Sen, "Design of a Single-Frequency Filter that Minimizes Ionosphere Divergence Error", *ION GNSS 2007.*

[9] M. Luo, S. Pullen, S. Datta-Barua, G. Zhang, T. Walter, and P. Enge, "LAAS Study of Slow-Moving Ionosphere Anomalies and Their Potential Impacts", *Institute of Navigation's GNSS Meeting*, September 2005

[10] M. Luo, S. Pullen, D. Akos, G. Xie, S. Datta-Barua, T. Walter, and P. Enge, "Assessment of Ionospheric Impact on LAAS Using WAAS Supertruth Data", Institute of Navigation's Annual Meeting, June 2002